


Proceedings Article

Role of Phase Encoding in Pulsed Magnetic Particle Imaging

Fabian Mohn ^{1,2,*}. Tobias Knopp ^{1,2}. Matthias Graeser ^{1,2,3,4}

¹Section for Biomedical Imaging, University Medical Center Hamburg-Eppendorf, Hamburg, Germany

²Institute for Biomedical Imaging, Hamburg University of Technology, Hamburg, Germany

³Fraunhofer Research Institute for Individualized and Cell-based Medicine, Lübeck, Germany

⁴Institute for Medical Engineering, University of Lübeck, Lübeck, Germany

*Corresponding author, email: f.mohn@uke.de

© 2021 Mohn *et al.*; licensee Infinite Science Publishing GmbH

This is an Open Access article distributed under the terms of the Creative Commons Attribution License (<http://creativecommons.org/licenses/by/4.0>), which permits unrestricted use, distribution, and reproduction in any medium, provided the original work is properly cited.

Abstract

Non-sinusoidal excitation waveforms have the ability to improve the signal-to-noise ratio and image resolution under certain conditions. Yet, the ability to use phase information for spatial encoding is expected to diminish as sharp pulses lead to concurrent signal response due to steep slopes and therefore less phase information. This motivates investigations into alternate sampling approaches that mitigate a loss in spatial encoding. However, measurements and image reconstruction results indicate that 10 times faster slew rates compared to sine excitation lead to enough phase information to resolve basic features using system matrix reconstruction.

1. Introduction

Most approaches to Magnetic Particle Imaging (MPI) rely on a superposition of sinusoidal excitation waveforms to generate static and dynamic magnetic fields, which result in a complex valued receive spectrum [1]. The system matrix approach to spatial encoding relies as much on amplitude as on phase of the receive spectrum to iteratively solve the underlying system of linear equations. The implementation of non-sinusoidal waveforms raises the question if phase information is lost due to fast slew rates and if this information is necessary to encode different tracer positions across the field of view (FOV). Motivated by recent improvements in resolution for large particles using pulsed excitation [2], this work compares sinusoidal and pulsed measurement data. So far, pulsed MPI has been specifically tailored to large particles with a long relaxation to overcome a blur (the relaxation wall) and follow the Langevin theory that predicts a better resolution for larger particles [2, 3]. However, pulsed excitation may also benefit a system matrix approach for

quick relaxing particles, by taking advantage of phase information when particles are able to follow the slew rate of the excitation waveform. This is a key benefit, as the signal phase is crucial for spatial encoding because it attributes a unique spectral fingerprint to each voxel. In the extreme case for pulsed excitation, the ideal rectangle, all phase information is lost, hence current approaches to spatial encoding become infeasible. This scenario is simulated in Fig. 1 for the one-dimensional case, that allows comparison of a sinusoidal, a rectangular and a sigmoid shaped excitation along a single line where exemplified particles are located in three different positions. The gradual excitation of a sinus allows a clear separation of different signal origins, however this information cannot be recovered for an ideal rectangular pulse because all signal contributions overlay. One solution to this loss of spatial information is an alternative approach to sequence design that may restore spatial information for pulsed excitations by a combination of shifts and rotations [4]. Real excitation waveforms have a shape more similar to a sigmoid function and some

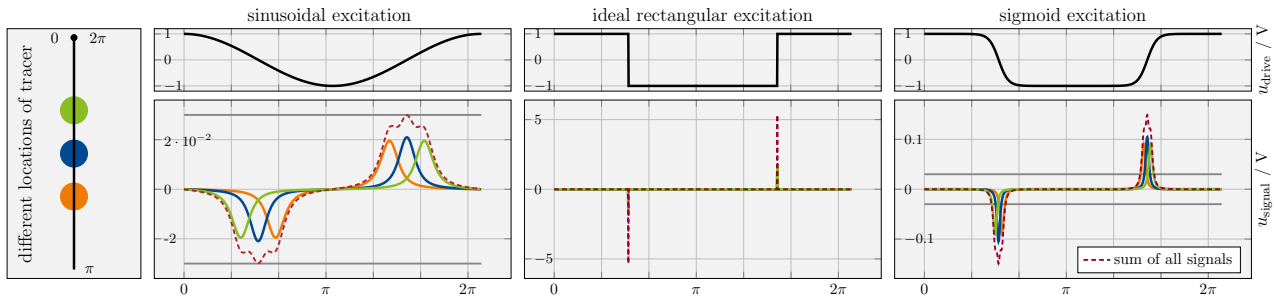


Figure 1: 1D simulations based on the Langevin function for different excitations. Plotted in different colors are signals originating from three distinct locations along a single line of excitation (left) over radian measure. Sinusoidal receive signals can be separated by their phase, whereas individual contributions are not distinguishable for an ideal rectangular pulse. The plot on the right depicts a more realistic pulsed excitation, where slew rates are limited by hardware. For reference between plots, a gray line is added indicating the maximum of the sum of all signals for the sinusoidal case.

phase information remains within the received signal spectrum as simulated in Fig. 1 on the right. Although the total induced signal is 5 times higher than the sinusoidal reference, a distinction in the time-shift of the three signal peaks is observable.

II. Methods

For measurements of pulsed excitations, a one-dimensional arbitrary waveform magnetic particle spectrometer (AWMPS) is used that can measure arbitrary waveforms with up to 20 mT in amplitude, superimposed by offsets in two dimensions [4, 5]. Two distinct system matrices are measured for each excitation type, one on a fine grid (0.5 mT steps) and another on a coarse grid (0.67 mT steps). In further effort to prevent inverse crime, two types of noise additions are performed: First during sequence generation, with

the 10-fold standard deviation to mask any repeating measurement background and in a second step during image reconstruction, where a realistic noise floor is added, measured from a pre-clinical MPI system [4]. For a fair comparison, different sequences are matched to have the same duration.

Measurements. All measurements are performed with a drive field frequency of 14.88 kHz with 15 mT amplitude and are transfer function (TF) corrected to gain device independence. Pulsed waveforms have a 3 μs rise time (slewrate 10 mT μs^{-1}). Raw data is reshaped into a single dataset, that contains offsets from two spatial dimensions. A selection of seven offsets in excitation direction x is plotted in Fig. 2 and the extrema of all offsets (0.5 mT steps) are displayed in Fig. 3, color-coded from negative (orange) to positive (green) offset values, with an offset-free curve for reference. The measured sample is a 20 μL sample with an iron concentration of 17 $\mu\text{g}_{\text{Fe}} \mu\text{L}^{-1}$ perimag (*micromod GmbH*, Rostock) to ensure a high measurement SNR.

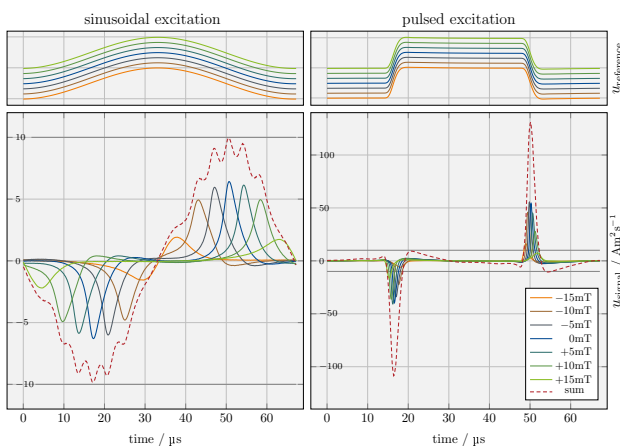


Figure 2: Measured signal response to a range of offsets. The top row contains the reference from a voltage monitor, the bottom row the corresponding TF corrected receive signal (same color) for a 15 mT excitation at 14.88 kHz.

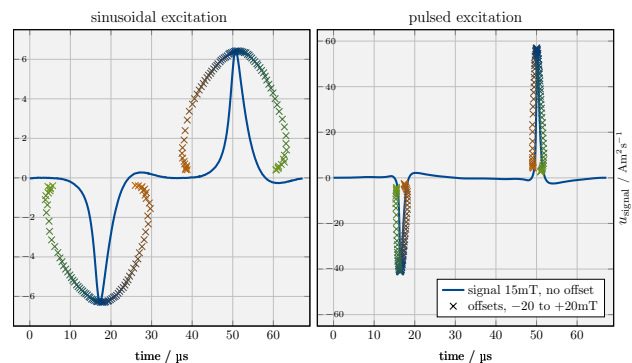


Figure 3: Positions of signal extrema are plotted over a range of offsets from -20 to 20 mT in 0.5 mT steps. For reference the 15 mT amplitude signal without offset is shown in blue. Orange corresponds to negative, green to positive offsets.

Sequence Generation. Two types of sequences are employed: One static sequence without any focus-field (FF) trajectory and a basic sequence with a Cartesian meandering FF trajectory, realized by shifts in x - and y -direction. The reason to create a sequence without any FF trajectory is to identify the resolution obtained by raw data phase information only. Due to its immobility, reconstructions based on this sequence type will not be able to resolve any phantom structures for an ideal rectangular pulse. The basic Cartesian trajectory uses an offset over-scan for extra space to shift the excitation in the manner of a focus-field, indicated by red lines in Fig. 4. The shift-amplitudes are 15 mT in y and 3 mT in x -direction, yielding a FOV of $36 \times 30 \text{ mT}^2$ due to the inherent x -amplitude of 15 mT.

Reconstructions. A concentration vector for phantom creation is generated by the fine gridded system matrix and a scaled phantom concentration distribution to match a target concentration of $5 \mu\text{g}_{\text{Fe}} \mu\text{L}^{-1}$. Reconstructed images are based on the coarse gridded system matrix with individual reconstruction parameters for each image using the iterative Kaczmarz method [6].

III. Results

Reconstructed images for sinusoidal and pulsed sequences without any FF trajectory are shown in Fig. 4 for two different phantoms. Additionally, results for a basic shifted FF trajectory with pulsed excitation are displayed on the right, which is able to resolve all fundamental phantom features. The FOV boundaries are indicated by dashed white lines, the FF trajectories are drawn with red lines. Pulsed excitation evokes a spatially broader response in y -direction from particles in saturation, which is indicated by the elliptic shape of the first row (no FF trajectory).

IV. Discussion and Conclusion

Reconstructed images in Fig. 4 indicate that the phase of pulsed raw data has almost the same ability to resolve basic features as a sinusoidal excitation, by comparing the immobile sequences without any FF trajectory. Edges have a superior representation for the sinusoidal data, probably benefiting from the broader spread of phase information. However, pulsed data only contains a fraction (10%) of the time-shift in signal peaks as shown in Fig. 3 and this phase seems sufficient for a system matrix reconstruction to restore basic features in proximity to the excitation line. The described basic trajectory is not expected to perform well for an ideal pulsed excitation without phase information, due to the fact that the unshifted amplitude covers 75% of the FOV. Thus, structures would appear strongly blurred. A smaller kernel

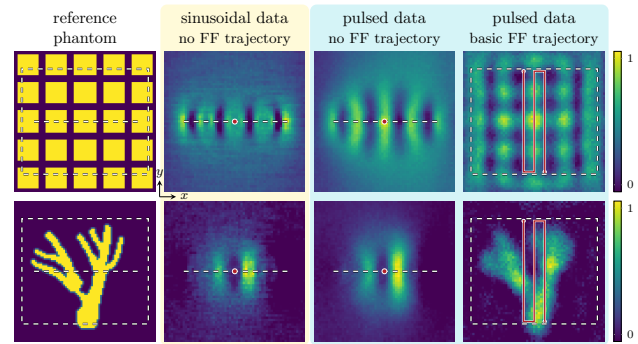


Figure 4: System matrix reconstructions of two phantoms. Columns 2 and 3 refer to a static sequence, that only relies on the excitation field. Consequently, the FOV is a single 30 mT line along its direction of excitation (x). White lines indicate FOV boundaries and red lines FF trajectories. Therefore, column 2 and 3 feature only a red dot with a dashed white line that indicates the 1D excitation, whereas in column 4 a focus field trajectory spans a 2D FOV. Sequence lengths are identical and images span $40 \times 40 \text{ mT}^2$.

with a broader trajectory would be required to restore finer resolution, for example by reducing the amplitude and increasing averages as done by Tay et. al [2]. Alternatively, a combination of shifts and rotations using large amplitudes is feasible [4]. Possible scenarios for a complete loss of phase information could either be an improved slew rate or measuring particles with a longer relaxation than perimag. The fact that the phase information for the chosen slew rates seem to provide enough spatial information for system matrix reconstructions is promising for simple Cartesian sampling schemes. Such sequences could be more successful than predicted, benefiting from the combination of high signal-to-noise ratio by large amplitudes and phase information from tracers with quick relaxation behaviour. Another aspect is the potential benefit for multi-contrast MPI, as the slew rate of an arbitrary waveform MPI system could be tailored to evoke response from one tracer, but not from a second. By determining individual particle characteristics and the limit where just sufficient phase information is obtained, one tracer could be rendered to lose phase information while another tracers maintains phase information. Such a separation could be exploited to distinguish multiple tracers.

Author's statement

Research funding: The authors thankfully acknowledge the financial support by the German Research Foundation (DFG, KN 1108/7-1 and GR 5287/2-1) The Fraunhofer IMTE is supported by the EU (EFRE) and the State Schleswig-Holstein, Germany (Project: IMTE – Grant: 124 20 002 / LPW-E1.1.1/1536. Conflict of interest: Authors state no conflict of interest.

References

- [1] B. Gleich and J. Weizenecker. Tomographic imaging using the non-linear response of magnetic particles. *Nature*, 435(7046):1214–1217, 2005, doi:[10.1038/nature03808](https://doi.org/10.1038/nature03808).
- [2] Z. W. Tay, D. Hensley, J. Ma, P. Chandrasekharan, B. Zheng, P. Goodwill, and S. Conolly. Pulsed Excitation in Magnetic Particle Imaging. *IEEE Transactions on Medical Imaging*, 38(10):2389–2399, 2019, Publisher: Institute of Electrical and Electronics Engineers (IEEE). doi:[10.1109/tmi.2019.2898202](https://doi.org/10.1109/tmi.2019.2898202).
- [3] Z. W. Tay, D. W. Hensley, E. C. Vreeland, B. Zheng, and S. M. Conolly. The relaxation wall: Experimental limits to improving MPI spatial resolution by increasing nanoparticle core size. *Biomedical Physics & Engineering Express*, 3(3):035003, 2017, Publisher: IOP Publishing. doi:[10.1088/2057-1976/aa6ab6](https://doi.org/10.1088/2057-1976/aa6ab6).
- [4] F. Mohn, T. Knopp, M. Boberg, F. Thieben, P. Szwargulski, and M. Graeser. System Matrix based Reconstruction for Pulsed Sequences in Magnetic Particle Imaging, _eprint: 2108.10073, 2021.
- [5] Z. W. Tay, P. W. Goodwill, D. W. Hensley, L. A. Taylor, B. Zheng, and S. M. Conolly. A High-Throughput, Arbitrary-Waveform, MPI Spectrometer and Relaxometer for Comprehensive Magnetic Particle Optimization and Characterization. *Scientific Reports*, 6, 2016, Publisher: Nature Publishing Group. doi:[10.1038/srep34180](https://doi.org/10.1038/srep34180).
- [6] T. Knopp, P. Szwargulski, F. Griese, M. Grosser, M. Boberg, and M. Möddel. MPIReco.jl: Julia package for image reconstruction in MPI. *International Journal on Magnetic Particle Imaging*, 5(1), 2019, doi:[10.18416/ijmpi.2019.1907001](https://doi.org/10.18416/ijmpi.2019.1907001).